STRUCTURAL CONTROL AND HEALTH MONITORING
Struct. Control Health Monit. 2011; **18**:79–98
Published online 12 October 2009 in Wiley Online Library (wileyonlinelibrary.com). DOI: 10.1002/stc.359

Parametric studies of the performance of particle dampers under harmonic excitation

Zheng Lu[1,2], Sami F. Masri[2,*,†] and Xilin Lu[1]

[1]*State Key Laboratory of Disaster Reduction, Civil Engineering, Tongji University, Shanghai 200092, China*
[2]*Viterbi School of Engineering, University of Southern California, Los Angeles, CA 90089-2531, U.S.A.*

SUMMARY

The performance of particle dampers under dynamic loads is very complicated and highly nonlinear; consequently, no guidelines currently exist for determining the optimum strategies for maximizing their behavior. The underlying interaction mechanics involve energy dissipation and momentum exchange. This paper presents the concept of 'effective momentum exchange' to quantify its influence on the performance of particle dampers with low volumetric filling ratio. The paper also evaluates the effects of a large number of system parameters (such as number, size and particle material, mass ratio, excitation frequency and amplitude level, coefficient of restitution, damping ratio of the primary system, and the coefficient of friction), using high-fidelity simulations based on the discrete-element method. It is shown that applying more particles with a high value of the coefficient of restitution can result in a broader range of acceptable response levels. For a given mass ratio, the particle type and size have minor effects on the primary system performance. Increasing the mass ratio can improve the damper's effectiveness but only up to a certain level. Friction is usually detrimental in low volumetric filling ratio particle dampers. It is shown that by using a properly designed particle damper, a lightly damped primary system can achieve a considerable reduction in its response with a small weight penalty. Copyright © 2009 John Wiley & Sons, Ltd.

Received 13 May 2009; Accepted 16 August 2009

KEY WORDS: particle damper; parametric study; discrete-element method; impact; momentum

1. INTRODUCTION

1.1. Background

While there are numerous passive devices for structural control applications (see, e.g. the works of Soong and Cimellaro [1], Fabio and Lucia [2], Markus and Franz [3], Gildin *et al.* [4], Ahmadizadeh [5] and Choi *et al.* [6]), a class of highly nonlinear dampers (particle dampers) that simultaneously utilize momentum transfer and internal energy dissipation offer some advantages in practical situations. Impact dampers [7], with their advantages of ruggedness, reliability, and insensitivity to extreme temperatures, are simple and efficient passive devices that are used to attenuate the vibrations of lightly damped structures, by momentum exchange and energy dissipation during the impact between solid particle and the primary system, to which they are attached. However, during the impact process, impulsive loads are transmitted between

*Correspondence to: Sami F. Masri, Viterbi School of Engineering, University of Southern California, Los Angeles, CA 90089-2531, U.S.A.
†E-mail: masri@usc.edu

the two coupled systems and will cause a high-level noise; simultaneously, large contact forces will result in material deterioration and local deformation accompanying plastic collisions. Furthermore, the performance of a single-particle impact damper may become sensitive to the coefficient of restitution, level and frequency of the excitation, as well as the container dimension. To reduce these problems, smaller size particles with the same mass ratio are used to replace the single solid particle, thus resulting in a potentially more efficient particle damper.

There is a long history of research in the modeling, analysis, simulation, design, and deployment of this class of vibration control devices. Masri [8–10] gave a closed solution for the steady-state motion of a multi-unit impact damper attached to a periodically excited primary system. Bapat and Sankar [11] studied the effect of Coulomb friction on the performance of identical multiunit impact damper. Popplewell and Semercigil [12] compared the performance of a resilient bean bag (a plastic bag filled with lead shots) and a conventional rigid impact damper under sinusoidal excitation. Bryce *et al*. [13] discussed the effectiveness and predictability of particle dampers and also developed a complete design methodology, which had been validated in laboratory. Xu *et al*. [14] confirmed the fact that shear friction in the longitudinal direction is effective as the major contributing mechanism of damping in the high volumetric packing ratio case. Bai *et al*. [15] proposed and investigated the behavior of a piston-based particle damper.

Many theoretical, numerical, and experimental studies have been carried out for the characterization of particle dampers [16]. Papalou and Masri [17–19] introduced an equivalent single-particle impact damper model to evaluate the performance of multi-particle dampers. Friend and Kinra [20] developed an analytical approach by treating multi particles as a lumped mass system. Liu *et al*. [21] used an equivalent viscous damping model to represent the nonlinearity, which was extracted from experimental results. Xu *et al*. [22] presented an empirical method for particle damping design. Fang and Tang [23] developed an improved analytical model by multiphase flow theory based on the previous work of Wu *et al*. [24]. Although these equivalent models or empirical-based studies have given many new insights, they are essentially phenomenological, and the results are difficult to extrapolate beyond their respective experimental conditions. Recently, a discrete-element method (DEM), which can take interactions between particles into account, has been used to perform limited studies of particle dampers [25–27].

Despite all these efforts, due to the system's high nonlinearity and the complexity with a large number of parameters, the understanding of particle damper mechanism has still not been well developed. Although it is generally understood that a dominant mechanism of particle damping is in the form of momentum exchange and energy dissipation, nevertheless, little quantitative analysis has been done. In fact, Mao *et al*. [25], Fang and Tang [23], and Wong *et al*. [28] do give quantitative analysis of particle damper with high volumetric filling ratio in vertical excitation in regard to energy dissipation mechanics (gravity makes the particles tend to rest on the floor of the container), the performance of particle dampers with low volumetric filling ratio under horizontal excitations, with respect to momentum exchange mechanics, have not thoroughly studied. Moreover, many parameters influence the behaviors of particle dampers; however, it is not feasible to investigate the numerous particle damper parameters experimentally. Hence, there is a need for a comprehensive study of influence of various system parameters on their performance.

1.2. Scope

This paper numerically investigates the performance of particle dampers in three dimensions under harmonic excitation through a large number of parametric studies. A new concept of effective momentum exchange (EME) is advanced to quantitatively characterize some of the physics of particle dampers. The contents of this paper are arranged as follows: Section 2 presents the governing equations of motion for a particle damper in three dimensions. A simulation program (PD3D) based on DEM is introduced. Section 3 validates the program in

DOI: 10.1002/stc

both special cases and experimental cases. In Section 4, the effect of different parameters, for example, number, size and particle material, mass ratio, excitation frequency and amplitude level, coefficient of restitution, damping ratio of the primary system, and the coefficient of friction, are studied. Additionally, the relationship between the performance of particle dampers and the EME is illustrated.

2. SIMULATION METHOD

The simplified model shown in Figure 1 represents a primary system equipped with a nonlinear auxiliary particle damper, in which a certain number of particles are placed. The whole system is positioned in the $x-y$ plane, and is excited by a harmonic excitation. By letting u and x be the harmonic displacement of the plane and the displacement of the primary system, respectively, the equation of motion for the primary system is:

$$\begin{aligned} &M\ddot{x} + k(x-u) + c(\dot{x}-\dot{u}) = F, \quad u = a\sin\omega t \quad \text{or} \\ &\ddot{x} = \omega_{\mathrm{n}}^2(u-x) + 2\zeta\omega_{\mathrm{n}}(\dot{u}-\dot{x}) + F/M, \quad u = a\sin\omega t \end{aligned} \tag{1}$$

where M, k, and c are the mass, equivalent stiffness, and damping constant of the primary system, respectively; F is the contact force acting on the primary system in the direction of the x-axis, a and ω are the amplitude and the angular frequency of the harmonic excitation, respectively; $\omega_{\mathrm{n}} = \sqrt{k/M}$ is the primary system natural frequency and $\zeta = c/2M\omega_{\mathrm{n}}$ is the primary system fraction of critical damping. The dimensions of the container of the primary system are dx (length), dy (width), and dz (height), which are parallel to the x, y, and z direction, respectively. The dots denote a time derivative.

The DEM [29] is applied to capture the behavior of the entire system in detail. With this technique, the positions and contact forces of particles and the primary system can be traced at every tiny time step. In this study, the *adhesive force* is neglected; consequently, the governing equation for a particle i can be written as

$$m_i\ddot{\mathbf{p}}_i = m_i\mathbf{g} + \sum_{j=1}^{k_i}(\mathbf{F}_{ij}^{\mathrm{n}} + \mathbf{F}_{ij}^{\mathrm{t}}) \tag{2}$$

$$\mathbf{I}_i\ddot{\varphi}_i = \sum_{j=1}^{k_i}\mathbf{T}_{ij} \tag{3}$$

where m_i is the mass of particle i, $\mathbf{I_i}$ is the moment of inertia of particle i, and $\mathbf{g}$ is the acceleration vector due to gravity; $\mathbf{p}_i$ is the position vector of the center of gravity of particle i, φ_i is the angular displacement vector, $\mathbf{F}_{ij}^{\mathrm{n}}$ is the normal contact force between particle i and

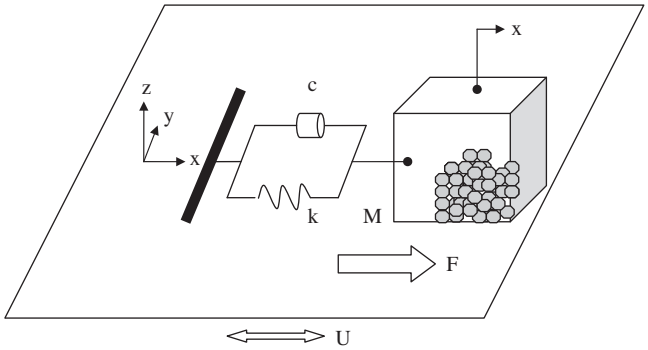

Figure 1. Model of the particle damper.

DOI: 10.1002/stc

particle j (if particle i is in contact with container wall, then j denotes that wall), and $\mathbf{F}_{ij}^{t}$ is the tangential contact force. The contact forces act at the contact point between particle i and particle j rather than the particle center, and they will generate a torque, $\mathbf{T}_{ij}$, causing particle i to rotate. For a spherical particle of radius r_i, $\mathbf{T}_{ij}$ is given by $\mathbf{T}_{ij} = r_i \mathbf{n}_{ij} \times \mathbf{F}_{ij}^{t}$, where $\mathbf{n}_{ij}$ is the unit vector from the center of particle i to the center of particle j and $\times$ denotes the cross product. These inter-particle forces are summed over the k_i particles in contact with particle i.

A number of contact models can be used to quantify the normal and tangential contact forces; however, this is still an active research topic, particularly for the tangential forces [30,31]. The present simulation study uses a linear contact model in the normal direction, and Coulomb's law of friction in the tangential direction.

Figure 2 presents the linear contact model between the particle and the wall in the normal direction, where k_2 is the stiffness of the impact damper 'stops', c_2 is the damping constant of the impact damper 'stops', and $\omega_2 = \sqrt{k_2/m}$ is the natural frequency, which can be used to simulate a rigid barrier to any degree of accuracy, by a proper choice. Based on previous studies [32], the ratio of $\omega_2/\omega_n \geqslant 20$ is appropriate to represent a 'stiff' barrier. $\zeta_2 = c_2/2m\omega_2$ is the fraction of critical damping, which can be used to simulate inelastic impacts, ranging from the completely plastic up to the elastic one, so the value of any desired coefficient of restitution can be adjusted by selecting the proper value for ζ_2. Similarly, k_3, ω_3, c_3, and ζ_3 in Figure 3 are the stiffness, natural frequency of spring and damping coefficient, and fraction of critical damping of the

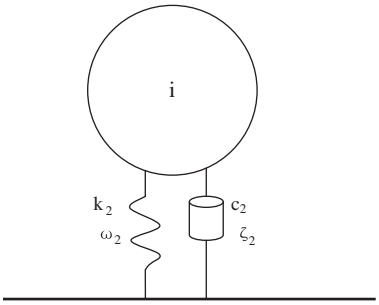

Figure 2. Normal contact force model between particle and wall.

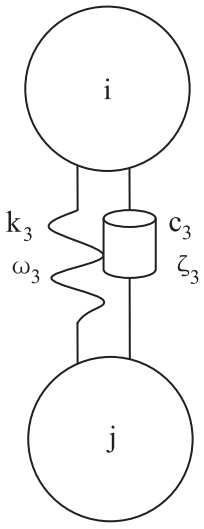

Figure 3. Normal contact force model between particle and particle.

DOI: 10.1002/stc

damper, respectively, in the inter-particle contact model along the normal direction. Hence, the normal contact force is expressed by

$$F_{ij}^{\mathrm{n}} = \begin{cases} k_2\delta_{\mathrm{n}} + 2\zeta_2\sqrt{mk_2}\dot{\delta}_{\mathrm{n}} & \delta_{\mathrm{n}} = r_i - t_i \quad \text{(particle}-\text{wall)} \\ k_3\delta_{\mathrm{n}} + 2\zeta_3\sqrt{\dfrac{m_i m_j}{m_i + m_j}k_3}\dot{\delta}_{\mathrm{n}} & \delta_{\mathrm{n}} = r_i + r_j - |\mathbf{p}_j - \mathbf{p}_i| \quad \text{(particle}-\text{particle)} \end{cases} \tag{4}$$

where δ_{n} and $\dot{\delta}_{\mathrm{n}}$ are the displacement and velocity of particle i relative to particle j, respectively, and t_i is the distance from the center of particle i to the wall.

Considering Coulomb's law of friction, the tangential contact force is expressed by

$$F_{ij}^{\mathrm{t}} = -\mu_s F_{ij}^{\mathrm{n}}\dot{\delta}_{\mathrm{t}}/|\dot{\delta}_{\mathrm{t}}| \tag{5}$$

where μ_s is the coefficient of friction between two particles or between a particle and the wall of the container, and $\dot{\delta}_{\mathrm{t}}$ is the velocity of particle i relative to particle j or the wall, in the tangential direction.

With the above in mind, the procedure for calculating the response of the particle dampers used in this study can now be illustrated. First, consider the relative position of the particles and walls. If $\delta_{\mathrm{n}} > 0$, the contact force acting on the particle can be determined from Equations (4) and (5); while if $\delta_{\mathrm{n}} \leqslant 0$, no contact force is produced. Secondly, sum all the contact forces acting on this particle, including inter-particle forces and particle-wall forces, if they exist. Thirdly, the particle motion can be analyzed by Equation (2) and (3). The same procedure is repeated for all the particles. Finally, the component of the contact force F acting on the primary system in the x-axis is given by the summation of all the contact forces between the particles and the wall of the container. By using the component of the contact force F, the equation of motion for the primary system, Equation (1) is analyzed.

As a part of the study reported herein, a code (PD3D) was programmed and implemented according to the above-mentioned procedures, and the fourth order *Runge-Kutta* method was applied to solve these ordinary differential equations.

3. SIMULATION MODEL EVALUATION

Two fundamental aspects are usually used to test a program model. The first one is to check that the code carries out what is specified in the model systems analysis, and the second one is to consider how valid the model is in comparison to the real world, which usually involves experiments.

3.1. Special tests

Several special cases were examined to check the asymptotic behavior of the model, and a summary of these validation tests is presented below.

3.1.1. Test 1: Normal elastic force, vertical. To test for the particle–wall impact case, the test simulates a free-falling particle under gravity hitting the floor of the container. Tangential forces and damping are set to zero. To test for the particle–particle force implementation, an identical test is conducted, but the particle impacts with a stationary particle instead of the floor of the container. The particle is dropped from the same height in both cases, as shown in Figure 4(a).

Since the particle is dropped from the same height, the results of both cases are identical. Figure 4(b) shows how in both cases the particle rebounds to its original height and the normal elastic force reaches a peak during contact. Note that no movement exists in the $x-y$ directions and no rotation occurs.

DOI: 10.1002/stc

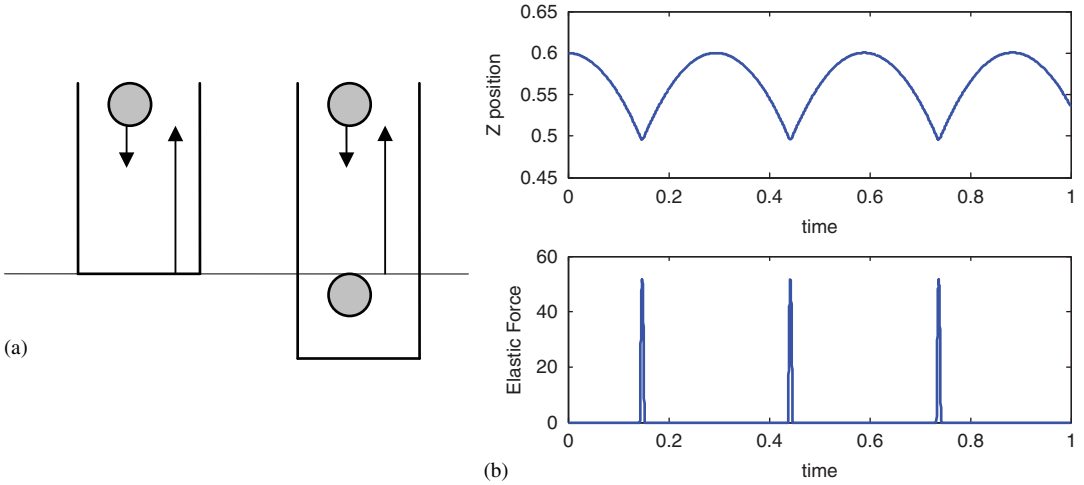

Figure 4. Test 1: Normal elastic force, vertical: (a) Schematic diagram and (b) Z position of the particle and elastic force.

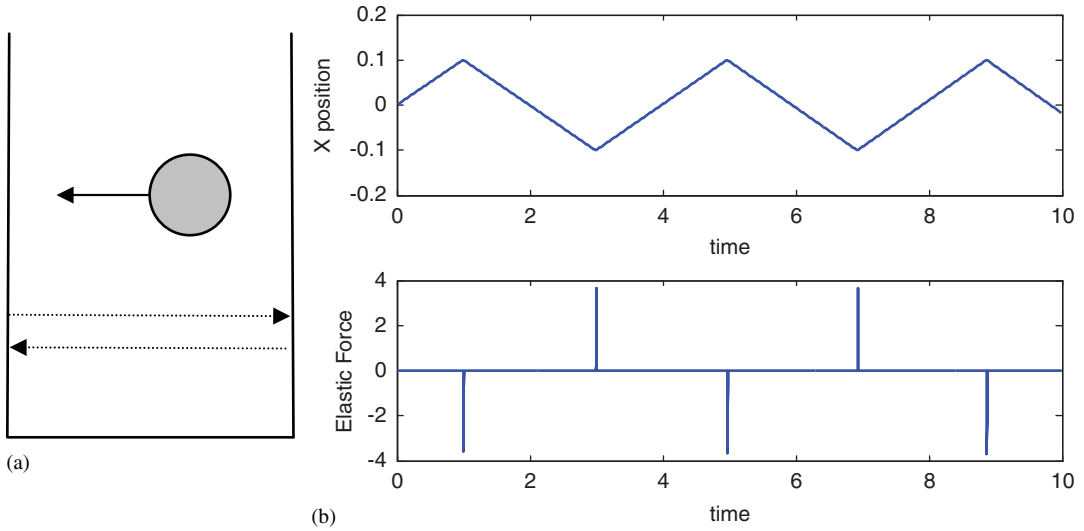

Figure 5. Test 2: Normal elastic force, horizontal: (a) Schematic diagram and (b) X position of the particle and elastic force.

3.1.2. Test 2: Normal elastic force, horizontal. This test is identical to Test 1, but with one particle moving with initial velocity either in the x- or y-direction. Gravitational, tangential, and damping forces are set to zero.

Figure 5(b) shows the results for a particle with initial velocity in the x-direction. As can be seen, the particle rebounds horizontally between the two walls of the container with no energy loss and the normal elastic force reaches a peak during contact. There is no movement in the $y-z$ directions and no rotation occurs.

3.1.3. Test 3: Normal damping force. This test is identical to Test 1, but with the normal damping force accounted for. The normal critical damping ratio used is 0.3. The schematic diagram can be referred to Figure 4(a).

Figure 6(a) shows how in both cases when the particle rebounds, it fails to reach the original height and its height decays due to damping, and finally it reaches a static equilibrium. Figure 6(c) shows the velocity immediately after the impact is smaller than that before the collision, until it becomes zero. Also, the normal elastic force and damping force at consecutive contacts are

DOI: 10.1002/stc

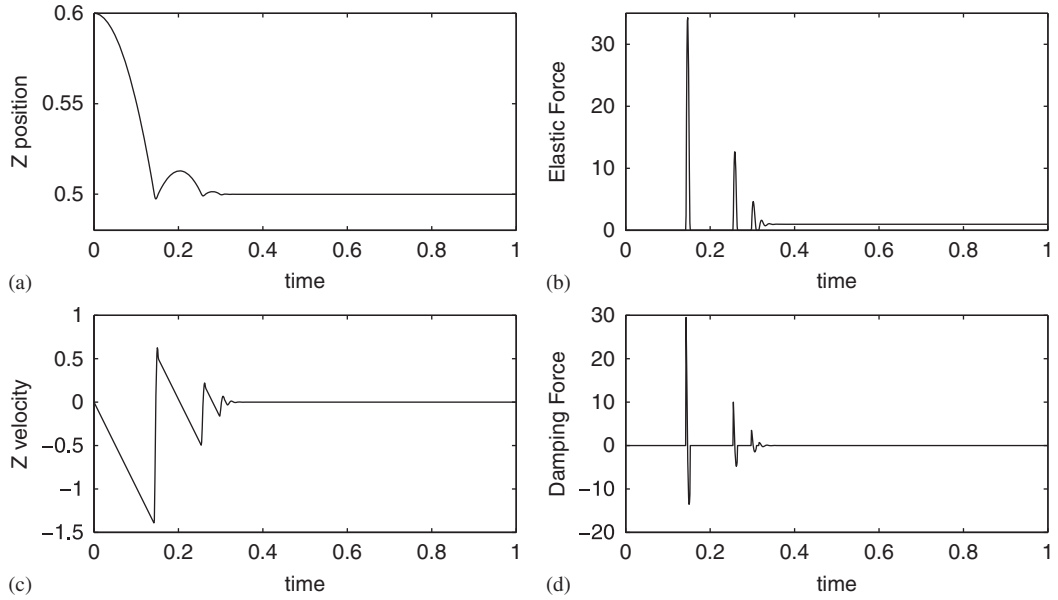

Figure 6. Test 3: (a) Z position of the particle; (b) Normal elastic force; (c) Z velocity of the particle; and (d) Normal damping force.

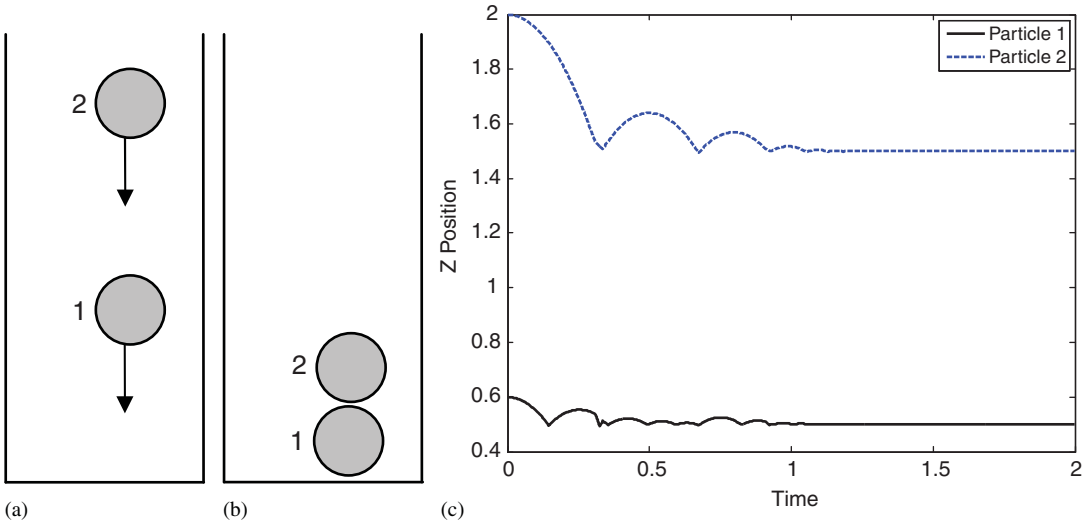

Figure 7. Test 4: Normal damping force with stacking: (a) Schematic diagram; (b) Stack diagram; and (c) Z position of particle 1 and particle 2.

successively less, as shown in Figure 6(b, d). There is no movement in the $x-y$ direction and no rotation.

3.1.4. Test 4: Normal damping force with stacking. This test is identical to Test 3 but with two particles dropped from different heights with zero initial velocity at the same time, as shown in Figure 7(a).

Figure 7(b) shows the final condition, in which the higher particle stacks on the lower particle in a column, and the lower particle rests on the ground. The separation between the lower particle and the ground is its radius, while that between two particles equals to the summation of their radii. This can also be found in Figure 7(c), which shows their position time histories. It also validates the normal interaction model between the particles.

DOI: 10.1002/stc

3.1.5. Test 5: Particle impacts two particles (walls) simultaneously. This test is designed to test the situation in which a particle collides with two initially stationary particles or walls at the same time. The particle 1 is placed in the center of a square container. It is used as the impacting particle, which has the same initial velocities in the x- and y- directions. Particle 2 and particle 3 are positioned besides particle 1 in the x- and the y- directions, as shown in Figure 8(a).

At the beginning, particle 1 impacts particle 2 and particle 3 simultaneously, then it moves back in the southwest direction until it reaches the south wall and the west wall at the same time. After collision with these two walls, the particle moves back along the northeast direction, which is the original track before the collision with walls. Hence, the track of particle 1 is a straight line in the diagonal direction, which is shown in Figure 8(b).

3.2. Comparison with experiments

Figure 9 shows the response of a one-unit-multi-particle damper with different mass ratios under a sinusoidal excitation. The schematic diagram could be referred to Figure 1. The

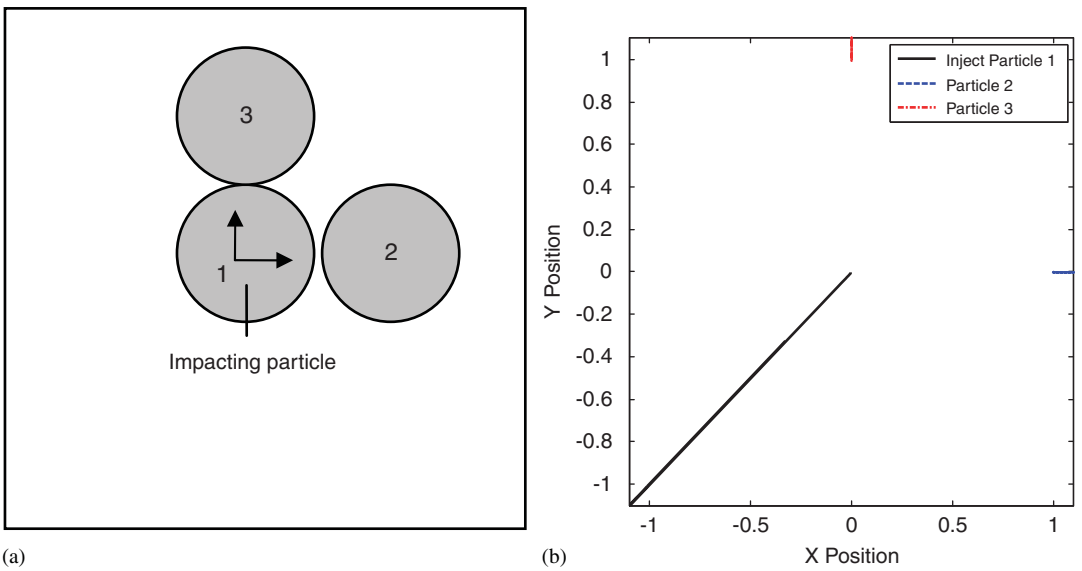

Figure 8. Test 5: Particle impacts with two particles (walls) simultaneously: (a) Schematic diagram and (b) $X-Y$ positions of particles.

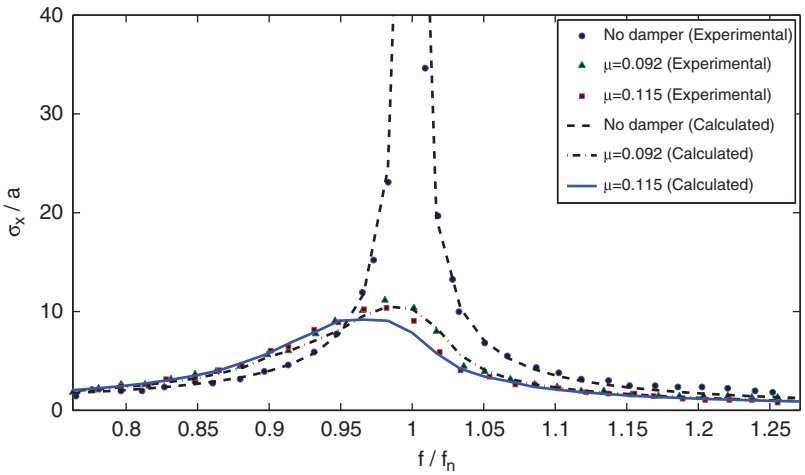

Figure 9. Comparison between experimental [26] and calculated (PD3D) results for a sinusoidally excited primary system provided with a one-unit-multi-particle damper, using the parameters in Table I.

DOI: 10.1002/stc

Table I. Values of system parameters in Figures 9 and 10.

Parameter	Figure 9	Figure 10
Unit number	1	5
Total particle number	200 ($\mu = 0.092$), 250 ($\mu = 0.115$)	192×5 ($\mu = 0.098$)
Diameter of the particle (m)	0.006	0.006
Density of the particle (kg/m^3)	1190	1190
Volumetric filling ratio	0.27 ($\mu = 0.092$), 0.34 ($\mu = 0.115$)	0.26 ($\mu = 0.098$)
Coefficient of friction	0.52	0.52
Critical damping ratio of the primary system	0.0027	0.0065
Critical damping ratio of the damper	0.1	0.1
Stiffness of the spring between particle and particle (N/m)	1.0×10^5	1.0×10^5
Stiffness of the spring between particle and wall (N/m)	1.3×10^5	1.3×10^5
Amplitude of excitation (m)	0.0005	0.0005

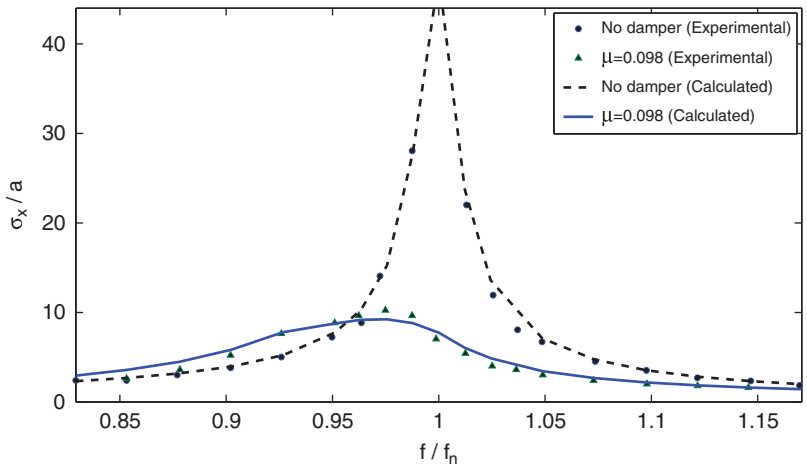

Figure 10. Comparison between experimental [27] and calculated (PD3D) results for a sinusoidally excited primary system provided with a multi-unit-multi-particle damper, using the parameters in Table I.

comparison between experimental results [26] and calculated results by PD3D is made. The root-mean-square value of the primary system displacement is made dimensionless by dividing σ_x by the amplitude of excitation, and the frequency of excitation is made dimensionless by dividing f by the primary system's natural frequency.

A multi-unit-multi-particle damper, which is composed of five cylindrical cavities with particles in them, was also investigated by Saeki [27], and the comparison between experimental and calculated results is displayed in Figure 10. The parameters used in the simulation can be found in Table I.

As can be seen from both figures, the calculated results agree well with the corresponding experimental results. Note that under harmonic excitation whose frequency is around the resonance frequency of the primary system, the ratio of maximum root-mean-square (r.m.s.) value of the displacement of the primary system with a particle damper and that without a particle damper (σ_x/σ_{x0}) will be used to quantify the effectiveness of the particle damper in the next section.

4. PARAMETRIC STUDY

In this section, parametric studies are performed on a single-degree-of-freedom structure with a particle damper under harmonic excitation to enhance the understanding of the particle damper behavior. Different system parameters such as gap clearance, number (N), size and material

DOI: 10.1002/stc

of particle, mass ratio (μ), excitation frequency and amplitude level, coefficient of restitution (e), damping ratio of the primary system, and coefficient of friction (μ_s) are investigated. In these simulations, the primary system natural frequency is 11.4 Hz, and the mass is 0.573 kg, dx is the separation of the walls of the damper that are perpendicular to the direction of the excitation, dy is the separation of the walls that are parallel to the direction of the excitation, and dz is the maximum height that the balls can reach. In order to get rid of the influence of transient vibration, the simulations are done for 250 periods of the primary system. The initial positions of the particles are distributed randomly so as to account for realistic situations where there is always a certain level of uncertainty in even nominally identical physical parameters.

Whether an impact damper reduces the response of the structure depends on how the particle and the system are moving relative to each other at the instant of impact, which can be separated into three types:

1. Type 1: The absolute velocities of both particle and the primary system are opposite to each other at the instant immediately before contact, which is the face-to-face impact.
2. Type 2: Although the particle and the primary system's absolute velocities have the same direction, the relative velocity of the particle is opposite prior to contact, which is the case for the primary system catching up with the particle.
3. Type 3: The particle and system's absolute velocities and the particle's relative velocity have the same direction just before contact, which is the case for the particle catching up with the primary system.

Collisions of Type 1 and Type 2 can reduce the response of the primary system, because a collision force, which is in the direction opposite to the velocity of the primary system, tends to prevent its moving. This kind of momentum exchange can be defined as 'useful momentum exchange' and this kind of impact can be called 'useful impact'. On the other hand, the collision of Type 3 is inclined to accelerate the primary system, thus such kind of momentum exchange is harmful to reduce the response of the primary system. Consequently, it is defined as 'harmful momentum exchange' and the impact is defined as 'harmful impact'. A new concept of EME is proposed herein to describe the combined effect of a useful momentum exchange minus a harmful momentum exchange. Based on a discussion in the following part, the EME can be seen to be very important in interpreting the physics involved in particle damper operation.

4.1. Effect of particle number, size, and material

These tests are conducted by keeping other parameters such as the level of excitation and the mass ratio constant. The mass ratio is defined by:

$$\mu = m/M = N\rho\pi d^3/6M \tag{6}$$

where ρ and d are the density and diameter of a particle, respectively. Consequently, for a given M, simultaneously changing two parameters of N, ρ, and d can result in the same μ.

4.1.1. Effect of particle size and number. This test keeps ρ as a constant and changes N and d, which is for the case of choosing to use a few large steel particles or many small steel particles in design process.

Figure 11 shows a sample results. Three curves overlap with each other in Figure 11(a), that is because in one particle damper case, the container dimension, which is perpendicular to the direction of excitation (dy), does not influence its behavior. As can be seen, for the small sizes of the container, the response amplitude is relatively high for all the

DOI: 10.1002/stc

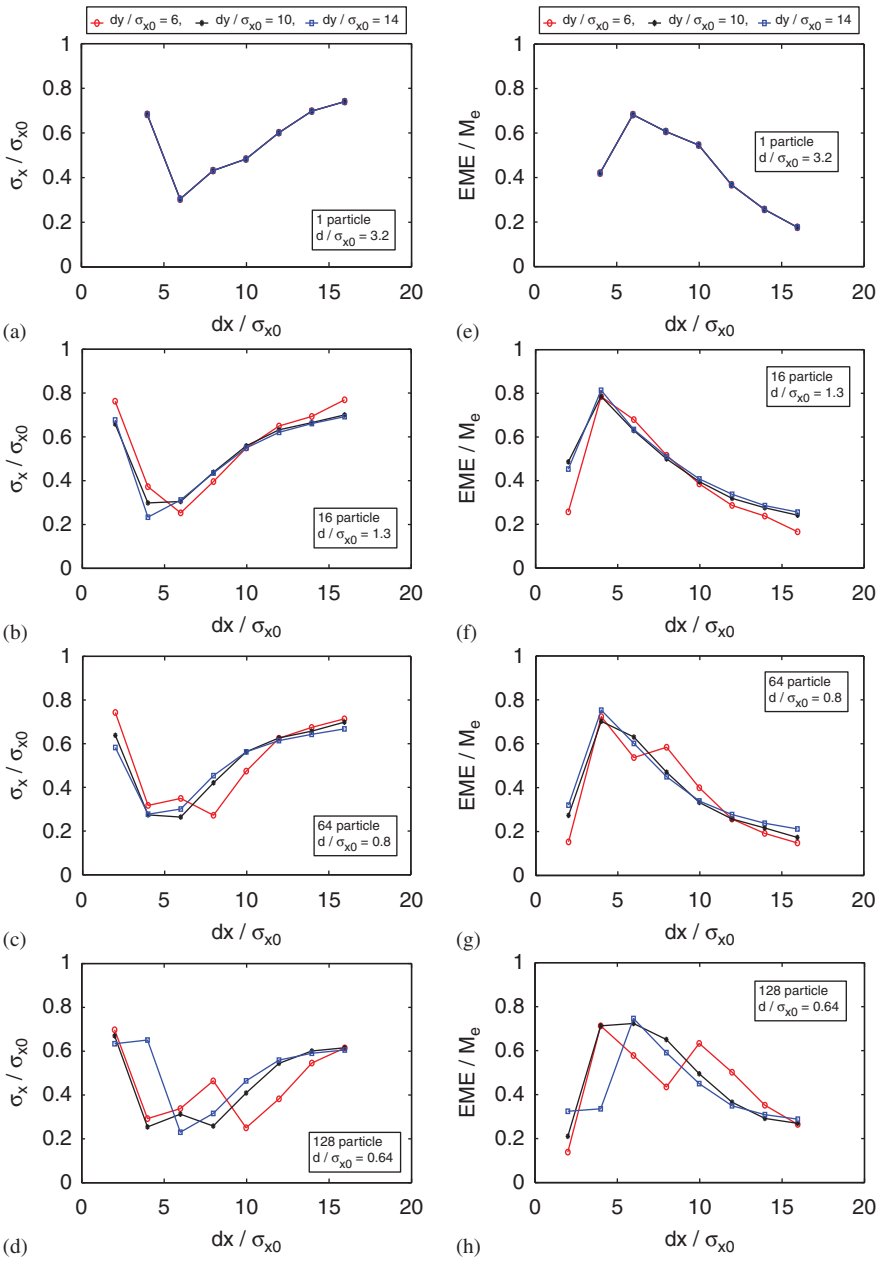

Figure 11. (a–d) R.M.S. response levels and (e–h) EME for the primary system with $\mu = 0.027$, $e = 0.75$, $\zeta = 0.004$, $\mu_s = 0.05$ (effect of particle number and size).

types of particles used. The reason for this behavior is that, when the dimensions of the damper are small, the particles are piled in many layers, which minimizes the motion of the lower layers and created a vigorous motion only in the top-most layers. The result is a smaller exchange of effective momentum and a corresponding decrease in the effectiveness of the damper.

For the middle sizes of the container, the response of the system is more sensitive to the particle size. As the particle size decreases, the sensitivity of vibration attenuation to changes in 'gap clearance' decreases, which results in a wider optimum margin of 'gap clearance'.

For large sizes of the container, the response amplitude is high for all particles used. This is due to the fact that a lot of energy is inefficiently extracted from the particles as they are hitting the walls that are parallel to the direction of excitation, or are not hitting any of the walls, which

DOI: 10.1002/stc

also decreases EME. Another reason may be that it takes a long time for particles to move from one wall that is perpendicular to the direction of excitation to the opposite wall after a collision, so relatively fewer impacts occur.

Another important observation from Figure 11 is that particle damper with more particles is slightly more effective in reducing the r.m.s. level of the response, as opposed to a single particle damper. However, there is not much difference in the best r.m.s. response level between the results of a 16- and a 128-particle damper, with the other parameters being the same. That is to say, a further increase of the number of particles above a certain number would not result in further response reduction. This phenomenon was also observed by Friend and Kinra [20] in their experiments.

If the corresponding EME is calculated, the above-mentioned phenomenon can be seen more clearly. Figure 11(e–h) shows the normalized version of EME, which is divided by the momentum exchange of the excitation force. In each case, a higher EME results in a better reduction of r.m.s. response amplitude. The highest points of EME in the 16- and the 128-particle cases are almost the same, so their maximum reductions are almost the same.

4.1.2. Effect of particle material and size. This test keeps N as a constant and changes ρ and d, which is for the case of choosing to use large plastic particles or small steel particles in design process.

All figures presented hereafter are for the same dy, which is $dy/\sigma_{x0} = 10$. The abscissa parameter in Figure 12(a) is normalized container length dx/σ_{x0}. It seems the optimum length gets smaller as particle size becomes smaller. However, as long as the particle size is small enough, the reduction will not change dramatically any more. That is because in the case for $d/\sigma_{x0} = 3.2$, one particle occupies a lot of space in dx direction, which is $d/dx = 0.8$ for the smallest dx and $d/dx = 0.2$ for the largest dx in Figure 12(a). If nominal 'gap clearance', which is $(dx - d)/\sigma_{x0}$, is plotted, different particle sizes make little difference in the reduction of the response of the primary system, as shown in Figure 12(b). This indicates that for the same mass ratio, particle impact damping is insensitive to the type and size of particles. Friend and Kinra [20] also present the same results in their experiments.

4.1.3. Effect of particle material and number. This test keeps d as a constant and changes ρ and N, which is for the case of choosing to use many plastic particles or a few steel particles in design process.

Figure 13(a) shows that for small sizes of the container, responses of the particle damper with a large number of particles are higher than that with small number of particles. The reason is that in

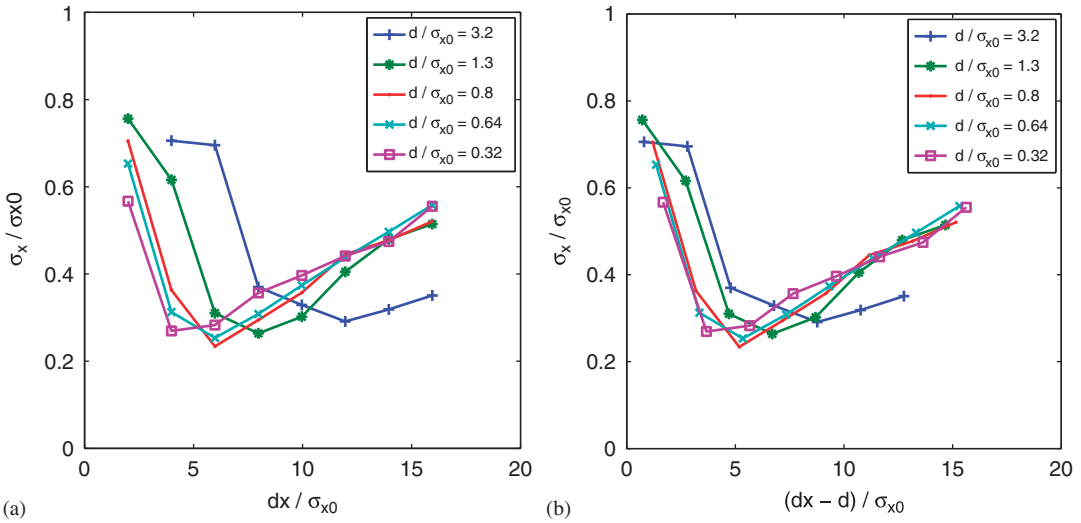

Figure 12. R.M.S. response levels for the primary system with $\mu = 0.027$, $e = 0.75$, $\zeta = 0.004$, $\mu_s = 0.05$ and 16 particles, versus (a) container length and (b) nominal 'gap clearance' (effect of particle material and size).

DOI: 10.1002/stc

the former case, particles will gather in many layers and lower layers are motionless. However, for large sizes of the container, they are reversed. In such cases, it takes a long time for a single particle traveling from one wall to the opposite wall, which makes fewer impacts. Increasing particle number can increase the possibility of the particle–wall collision. Hence, both optimum range of the container dimension and the efficiency of the particle damper are enhanced.

Figure 13(b) shows the corresponding volumetric filling ratios, which is the fraction of the total volume of all particles and the volume of the container. As can be seen, the ratios for all cases are generally small, that is because a relatively large dz is used in the simulation to get rid of the influence of particles hitting the roof. One can notice that for one-particle and two-particle cases, the volumetric filling ratios are quite small, and this is the reason why they perform better than 128-particle case. In fact, particles are gathered in three layers in 128-particle case for the smallest dx.

The above results clearly indicate that the number of particles plays a very important role in the behavior of a particle damper, given the same mass ratio. Applying more particles, even though the best attenuation of the r.m.s. response level cannot be improved, the optimum range of clearance can be broadened. On the other hand, the particle type and size have minor effects on the primary system performance.

4.2. *Effect of container dimensions*

It is certain that the r.m.s. response level for the particle damped system exhibits a minimum value for a certain clearance ratio, as shown in Figure 14(a). The corresponding EME is shown

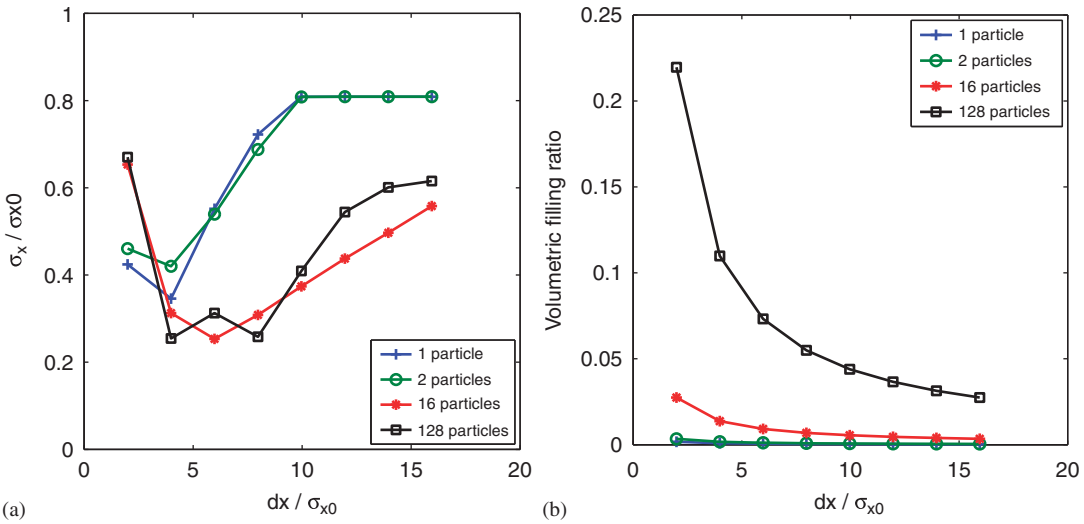

Figure 13. (a) R.M.S. response levels and (b) volumetric filling ratios for the primary system with $\mu = 0.027$, $e = 0.75$, $\zeta = 0.004$, $\mu_s = 0.05$ and $d/\sigma_{x0} = 0.64$ (effect of particle material and number).

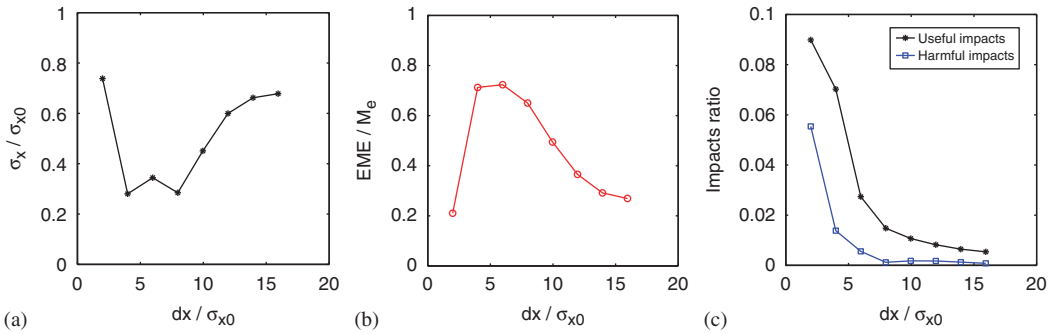

Figure 14. (a) R.M.S. response levels; (b) EME; (c) Impacts ratios for the primary system with $\mu = 0.027$, $e = 0.75$, $\zeta = 0.004$, $\mu_s = 0.05$, $d/\sigma_{x0} = 0.64$ and 128 particles (effect of container dimensions).

DOI: 10.1002/stc

in Figure 14(b). In Figure 14(c), 'useful impacts' and 'harmful impacts' are compared in nondimensional manner by dividing them by total impacts, including both particle–wall impacts and particle–particle impacts. One can see that both 'useful impacts' and 'harmful impacts' are only a small fraction of the total impacts. However, if these two are compared with each other, one can find that small container dimensions cause a large number of collisions, but accompanied by many harmful impacts, too. While in large container dimension cases, although the harmful impacts decreases, or even does not exist, a small number of impacts takes place, since the particles do not acquire enough momentum and have longer travel time. Both situations lead to low EME.

4.3. Effect of mass ratio

As shown in Equation (6), three basic methods can be used to investigate the effect of mass ratio:

1. Keeping ρ and d as constants and changing N, which is the case for having the same material and size of the particles, but using more identical particles.
2. Keeping ρ and N as constants and changing d, which is the case for having the same material and number of the particles, but using larger size.
3. Keeping d and N as constants and changing ρ, which is the case for having the same number and size of the particles, but using heavier ones.

Figure 15(a) shows that increasing the mass ratio of particles can reduce the response of the primary system, but the reduction is not directly proportional to the increase in mass ratio. Figure 15(b) depicts the minimum σ_x/σ_{x0}, which means the most reduction that a particle damper can get under the optimum choice of system parameters strategy. It shows that the effectiveness per unit mass ratio will decrease in a nonlinear manner as the mass ratio increases. Moreover, the optimum values of reduction are almost the same, given a certain mass ratio, no matter which basic method is used to increase μ.

Another interesting observation is that indefinitely increasing the mass of the particles may not reduce the response any further, especially for large sizes of the container. This phenomenon can be explained by considering the conservation of momentum between the particles and the system. As a specific particle's mass increases, its absolute velocity immediately after the impact decreases, which, in turn, reduces its relative velocity, and it takes a longer time to travel towards the other wall of the container. The force of friction also contributes to the reduction in the velocity while the particle is in motion. As the mass is increased beyond a certain value, its relative velocity immediately after the impact does not allow it to overcome the frictional force while in motion, and it comes to rest relative to the system prior to reaching the other wall. At that point, if the system resumes its motion in the same direction and its acceleration is large enough to overcome the force of friction, the particle starts traveling in the opposite direction relative to the system. If a similar situation arises prior to getting to the other container's boundary, the

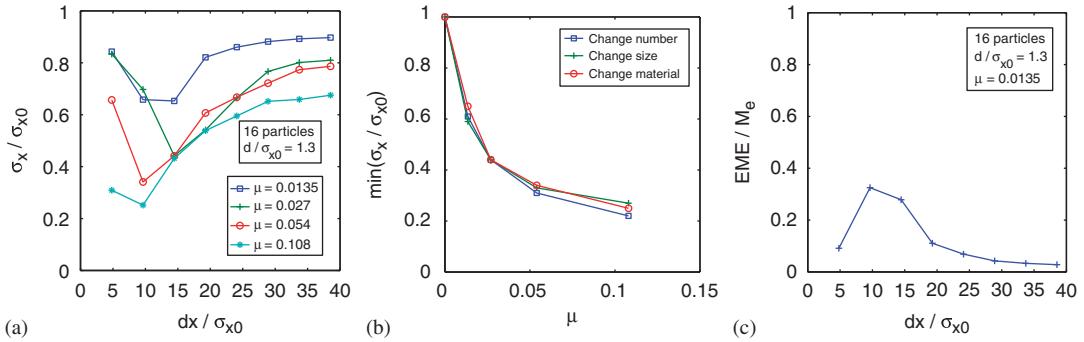

Figure 15. (a) R.M.S. response levels; (b) Minimum R.M.S. response levels versus μ; (c) EME for the primary system with $e = 0.75$, $\zeta = 0.01$, and $\mu_s = 0.05$ (effect of mass ratio).

DOI: 10.1002/stc

particle reverses its direction once again. It is possible for the particle to reciprocate between the container's boundaries, while the system goes through several cycles of motion before making the next impact. This phenomenon is also addressed by Butt in his experiments [33]. From Figure 15(c), one can find the EME decreases to a certain low level in large container dimensions.

4.4. *Effect of excitation frequency and amplitude level*

In the validation Section 3.2, Figures 9 and 10 show the influence of the excitation frequency. As can be seen, a particle damper can suppress structural resonant conditions over a wide frequency range, with a small weight penalty. The reduced peak r.m.s. amplitude of the primary system with particle damper occurs at a lower frequency compared with that without a particle damper, due to the added mass of particles.

Because of the highly nonlinear nature of particle dampers, the level of excitation plays a very important role. As the level of excitation increases, the efficiency of the damper increases due to the fact that the more energetic motion of the particles increase the exchange of momentum. On the other hand, when the excitation is high enough to mobilize all the particles, the response amplitude becomes independent of the intensity of the excitation, provided the dimensionless clearance ratio is maintained constant, as shown in Figure 16.

4.5. *Effect of coefficient of restitution*

Figure 17 shows that higher e's lead to a less reduction of the primary system's response in small-size containers, while a more reduction in large-size containers, compared to lower e's. The reason is that higher e can get a higher relative velocity immediately following the impact, which results in more collisions under a small clearance. In these collisions, much harmful momentum exchange happens and the EME is reduced. This also explains why the optimum clearance is increased as e increases. Another significant observation that can be gleaned from Figure 17 is that the sensitivity of a particle damper to changes in dx increases as e decreases, which results in the narrower optimum clearance for smaller e's. Consequently, a particle damper designed with a relatively high value of e can tolerate a broader range of excitation

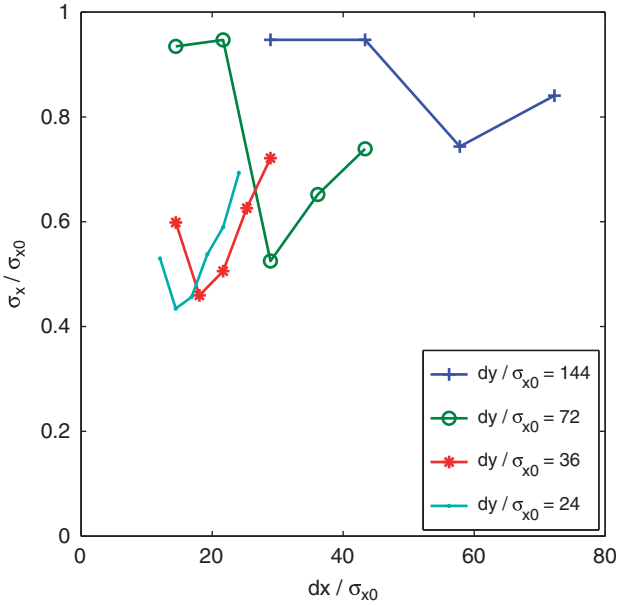

Figure 16. R.M.S. response levels for the primary system with $\mu = 0.027$, $e = 0.75$, $\zeta = 0.01$, $\mu_s = 0.05$, $d/\sigma_{x0} = 1.3$ and 16 particles (effect of excitation amplitude level).

DOI: 10.1002/stc

levels, while still performing around the optimum level. This phenomenon is also observed by Ramachandran [34].

4.6. *Effect of primary system damping*

Figure 18(a) shows that the effectiveness of the damper increases as the primary system damping decreases. Consequently, the maximum effect of a particle damper would be achieved for a primary system with a negligible amount of inherent damping. Figure 18(b) illustrates clearly the significant variation of the EME level for different ζ.

4.7. *Effect of primary system damping and mass ratio*

Figure 19 summarizes the effects of mass ratio and primary system damping on the optimum performance of a particle damper. It is clear that for a given ζ, the optimum response reduction

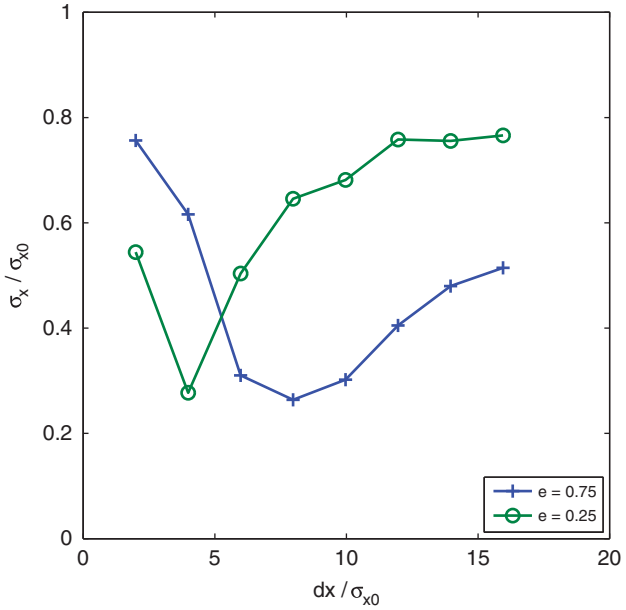

Figure 17. R.M.S. response levels for the primary system with $\mu = 0.027$, $\zeta = 0.004$, $\mu_s = 0.05$, $d/\sigma_{x0} = 1.3$ and 16 particles (effect of coefficient of restitution).

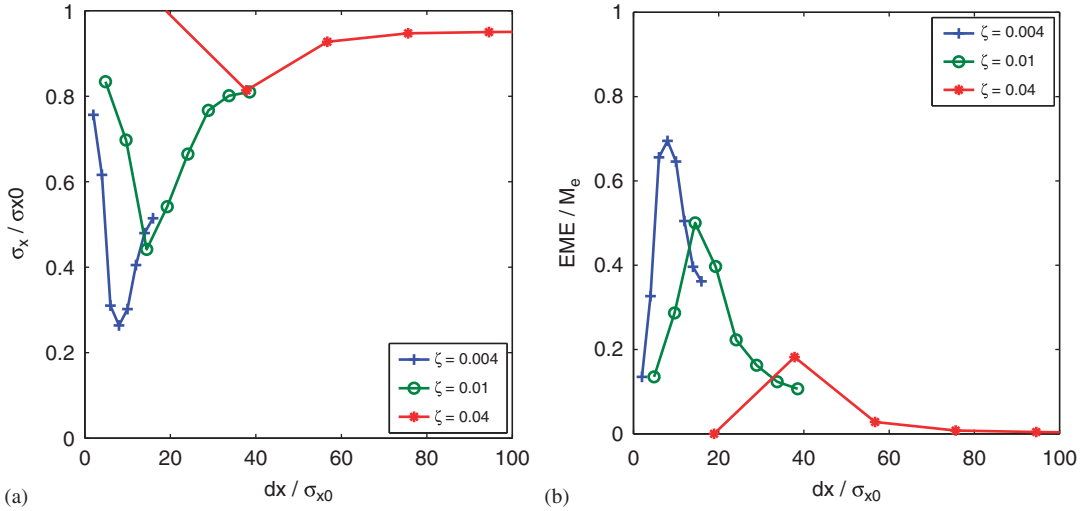

Figure 18. (a) R.M.S. response levels; (b) EME for the primary system with $\mu = 0.027$, $e = 0.75$, $\mu_s = 0.05$, $d/\sigma_{x0} = 1.3$ and 16 particles (effect of primary system damping).

DOI: 10.1002/stc

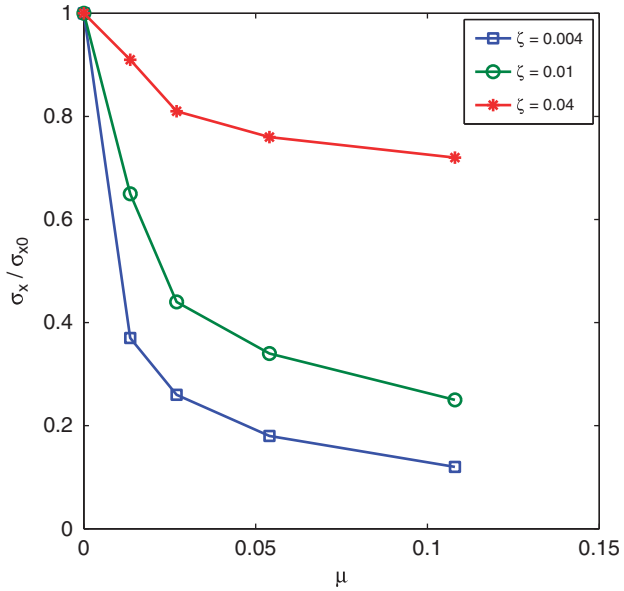

Figure 19. Effect of primary system damping and mass ratio on the performance of particle damper with $e = 0.75$, $\mu_s = 0.05$, $d/\sigma_{x0} = 1.3$ and 16 particles.

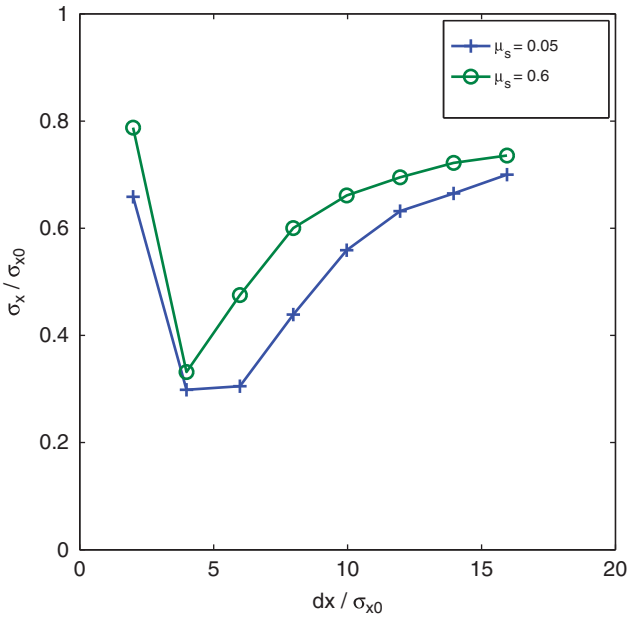

Figure 20. R.M.S. response levels for the primary system with $\mu = 0.027$, $e = 0.75$, $\zeta = 0.004$, $d/\sigma_{x0} = 1.3$ and 16 particles (effect of coefficient of friction).

is not a linear function of the mass ratio. Also, one can conclude that even with very small mass ratios, a properly designed particle damper is capable of substantial attenuation of the r.m.s. response level.

4.8. Effect of coefficient of friction

Figure 20 shows that a particle damper with a small coefficient of friction can get more r.m.s. level reduction compared to that with a large coefficient of friction. This is because small friction results in more energetic motions of particles and the primary system has more momentum

DOI: 10.1002/stc

exchange. Although large friction can dissipate more energy during sliding and impacting, the collision times and momentum exchange are relatively smaller, especially for the small volumetric filling ratio case. This phenomenon can also be found in Bapat's paper [11].

5. SUMMARY AND CONCLUSION

Although Papalou and Masri [17–19] have presented the results of many experiments with particle dampers under dynamic loads, the performance of such nonlinear devices is a highly complex nonlinear process involving energy dissipation and momentum exchange, and is not amenable to exact analytical solutions. Consequently, there are no guidelines currently existing for determining the optimum strategies for maximizing the performance of particle dampers under dynamic loads.

This paper further evaluates the effects of system parameters (such as the number, size and material of particles, mass ratio, excitation frequency and amplitude level, coefficient of restitution, damping ratio of the primary system, and the coefficient of friction) on the performance of particle dampers under harmonic excitation. High-fidelity simulations based on the DEM are conducted, validated, and interpreted.

It is shown that a quantity termed the EME is useful in characterizing the essential operational features of particle dampers, with low volumetric filling ratio, under horizontal vibration. The optimum range of clearance can be broadened if more particles are applied, although the best vibration attenuation cannot be improved. The particle type and size have minor effects on the impact damping capability. Increasing the mass ratio results in a proportionally nonlinear decrease of the response amplitude up to a certain limit. As long as the excitation severity is high enough to mobilize all the particles, the primary system response amplitude becomes independent of the intensity of the excitation. A relatively high value of the coefficient of restitution can result in a wider range of excitation levels. The effect of friction on the performance is generally detrimental in the case of low volumetric filling ratio. Through a properly designed particle damper, a lightly damped primary system can achieve a considerable reduction in the response with small weight penalty.

NOMENCLATURE

φ_i	angular displacement vector of particle i
δ_{n}	normal relative displacement
$\dot{\delta}_{\mathrm{n}}$	normal relative velocity
$\dot{\delta}_{\mathrm{t}}$	tangential relative velocity
$\mathbf{F}_{ij}^{\mathrm{n}}$	normal contact force between particle i and particle j
$\mathbf{F}_{ij}^{\mathrm{t}}$	tangential contact force between particle i and particle j
$\mathbf{g}$	acceleration vector due to gravity
$\mathbf{I_i}$	moment of inertia of particle i
$\mathbf{n}_{ij}$	unit vector from the center of particle i to the center of particle j
$\mathbf{p}_i$	position vector of the center of gravity of particle i
$\mathbf{T}_{ij}$	torque between particle i and particle j
μ	mass ratio, which is the ratio of the total mass of particles and the mass of the primary system
μ_s	coefficient of friction
ω	angular frequency of the harmonic excitation
ω_2	natural frequency of the impact damper 'stops'
ω_3	natural frequency of the spring between two particles
ω_{n}	natural frequency of the primary system
ρ	density of a particle
σ_{x0}	maximum root-mean-square value of the displacement of the primary system without a particle damper

DOI: 10.1002/stc

σ_x maximum root-mean-square value of the displacement of the primary system with a particle damper
ζ critical damping ratio of the primary system
ζ_2 critical damping ratio of impact damper 'stops'
ζ_3 critical damping ratio of the damper between two particles
a amplitude of the harmonic excitation
c damping constant of the primary system
c_2 damping constant of impact damper 'stops'
c_3 damping constant of the damper between two particles
d diameter of a particle
dx separation of the walls of the damper that are perpendicular to the direction of the excitation (length of the container)
dy separation of the walls of the damper that are parallel to the direction of the excitation (width of the container)
dz maximum height that the particles can reach (height of the container)
e coefficient of restitution
F contact force acting on the primary system by particles
k equivalent stiffness of the primary system
k_2 stiffness of the impact damper 'stops'
k_3 stiffness of the spring between two particles
k_i number of contact particles that are in contact with particle i
M mass of the primary system
m_i mass of the particle i
N total number of the particles
t_i distance from the center of particle i to the wall

ACKNOWLEDGEMENTS

Financial supports from the National Natural Science Foundation of China through grant 90815029 is highly appreciated. Financial support from the China Scholarship Council for the first author's work at the University of Southern California as a visiting scholar is gratefully acknowledged.

REFERENCES

1. Soong T, Cimellaro GP. Future directions in structural control. *Structural Control and Health Monitoring* 2009; **16**(1):7–16.
2. Casciati F, Faravelli L. A passive control device with sma components: from the prototype to the model. *Structural Control and Health Monitoring* 2009; **9999**.
3. Markus JH, Ziegler F. Control of tall building vibrations by sealed tuned liquid column dampers. *Structural Control and Health Monitoring* 2006; **13**(6):980–1002.
4. Gildin E, Antoulas AC, Sorensen D, Bishop RH. Model and controller reduction applied to structural control using passivity theory. *Structural Control and Health Monitoring* 2009; **16**(3):319–334.
5. Ahmadizadeh M. On equivalent passive structural control systems for semi-active control using viscous fluid dampers. *Structural Control and Health Monitoring* 2007; **14**(6):858–875.
6. Choi KM, Jung HJ, Lee HJ, Cho SW. Seismic protection of base-isolated building with nonlinear isolation system using smart passive control strategy. *Structural Control and Health Monitoring* 2008; **15**(5):785–796.
7. Masri SF, Caughey TK. On the stability of the impact damper. *Journal of Applied Mechanics* 1966; **33**(3):586–592.
8. Masri SF. Effectiveness of two-particle impact dampers. *Journal of the Acoustical Society of America* 1967; **41**(6):1553–1554.
9. Masri SF. Analytical and experimental studies of multiple-unit impact dampers. *Journal of the Acoustical Society of America* 1969; **45**(5):1111–1117.
10. Masri SF. General motion of impact dampers. *Journal of the Acoustical Society of America* 1970; **47**(1P2):229–237.
11. Bapat CN, Sankar S. Multiunit impact damper—reexamined. *Journal of Sound and Vibration* 1985; **103**(4):457–469.
12. Popplewell N, Semercigil SE. Performance of the bean bag impact damper for a sinusoidal external force. *Journal of Sound and Vibration* 1989; **133**(2):193–223.
13. Bryce LF, Eric MF, Steven EO. Effectiveness and predictability of particle damping. *Smart Structures and Materials 2000*: *Damping and Isolation*, vol. 3989(1), 2000; 356–367.

DOI: 10.1002/stc

14. Xu ZW, Wang MY, Chen TN. An experimental study of particle damping for beams and plates. *Journal of Vibration and Acoustics Transactions of the ASME* 2004; **126**(1):141–148.
15. Bai XM, Shah B, Keer LM, Wang QJ, Snurr RQ. Particle dynamics simulations of a piston-based particle damper. *Powder Technology* 2009; **189**(1):115–125.
16. Ibrahim RA. *Vibro-Impact Dynamics*, *Modeling*, *Mapping and Applications*, vol. 43. Springer: Berlin, Heidelberg, 2009.
17. Papalou A, Masri SF. Performance of particle dampers under random excitation. *Journal of Vibration and Acoustics Transactions of the ASME* 1996; **118**(4):614–621.
18. Papalou A, Masri SF. Response of impact dampers with granular materials under random excitation. *Earthquake Engineering and Structural Dynamics* 1996; **25**(3):253–267.
19. Papalou A, Masri SF. An experimental investigation of particle dampers under harmonic excitation. *Journal of Vibration and Control* 1998; **4**(4):361–379.
20. Friend RD, Kinra VK. Particle impact damping. *Journal of Sound and Vibration* 2000; **233**(1):93–118.
21. Liu W, Tomlinson GR, Rongong JA. The dynamic characterisation of disk geometry particle dampers. *Journal of Sound and Vibration* 2005; **280**(3–5):849–861.
22. Xu ZW, Chan KW, Liao WH. An empirical method for particle damping design. *Shock and Vibration* 2004; **11**(5–6):647–664.
23. Fang X, Tang J. Granular damping in forced vibration: qualitative and quantitative analyses. *Journal of Vibration and Acoustics Transactions of the ASME* 2006; **128**(4):489–500.
24. Wu CJ, Liao WH, Wang MY. Modeling of granular particle damping using multiphase flow theory of gas-particle. *Journal of Vibration and Acoustics Transactions of the ASME* 2004; **126**(2):196–201.
25. Mao KM, Wang MY, Xu ZW, Chen TN. DEM simulation of particle damping. *Powder Technology* 2004; **142**(2–3):154–165.
26. Saeki M. Impact damping with granular materials in a horizontally vibrating system. *Journal of Sound and Vibration* 2002; **251**(1):153–161.
27. Saeki M. Analytical study of multi-particle damping. *Journal of Sound and Vibration* 2005; **281**(3–5):1133–1144.
28. Wong CX, Daniel MC, Rongong JA. Energy dissipation prediction of particle dampers. *Journal of Sound and Vibration* 2009; **319**(1–2):91–118.
29. Cundall PA, Strack ODL. A distinct element model for granular assemblies. *Geotechnique* 1979; **29**:47–65.
30. Di Renzo A, Di Maio FP. Comparison of contact-force models for the simulation of collisions in DEM-based granular flow codes. *Chemical Engineering Science* 2004; **59**(3):525–541.
31. Elperin T, Golshtein E. Comparison of different models for tangential forces using the particle dynamics method. *Physica A* 1997; **242**(3–4):332–340.
32. Masri SF. Steady-state response of a multidegree system with an impact damper. *Journal of Applied Mechanics Transaction of the ASME* 1973; **40**(1):127–132.
33. Butt AS. Dynamics of impact-damped continuous systems. *Ph.D. Dissertation*, Louisiana Tech University, Louisiana, 1995.
34. Ramachandran S, Lesieutre G. Dynamics and performance of a harmonically excited vertical impact damper. *Journal of Vibration and Acoustics Transactions of the ASME* 2008; **130**(2):11. DOI: 10.1115/1.2827364.